Phase behaviour of the solid proton conductor $CsHSO_4$

2006 J. Phys.: Condens. Matter 18 9561

(http://iopscience.iop.org/0953-8984/18/42/003)

INSTITUTE OF PHYSICS PUBLISHING JOURNAL OF PHYSICS: CONDENSED MATTER

J. Phys.: Condens. Matter **18** (2006) 9561–9573 doi:10.1088/0953-8984/18/42/003

Phase behaviour of the solid proton conductor $CsHSO_4$

E Ortiz[1], R A Vargas[2] and B-E Mellander[3]

[1] Department of Physics, Universidad del Atlántico, A. A. 1890, Barranquilla, Colombia
[2] Department of Physics, Universidad del Valle, A. A. 25360, Cali, Colombia
[3] Department of Applied Physics, Chalmers University of Technology, SE-41296 Göteborg, Sweden

E-mail: eortiz@uniatlantico.edu.co, eortizmunoz@hotmail.com, rvargas@univalle.edu.co and f5xrk@fy.chalmers.se (B-E Mellander)

Received 26 August 2006, in final form 15 September 2006
Published 5 October 2006
Online at stacks.iop.org/JPhysCM/18/9561

Abstract

The sequence of previously found phase transitions in $CsHSO_4$ at around 60, 122, and 141 °C was carefully examined by using thermo-gravimetric analysis (TGA), mass spectroscopy (MS), differential thermal analysis, ac calorimetry, impedance spectroscopy, and x-ray diffraction (XRD). Our results show evidence that at all these transition temperatures, the dehydration processes take place at or very near the surface of the crystal. As a consequence, our results support the phase of $CsHSO_4$ above 141 °C being not a superprotonic-conducting phase but rather a mixture of $CsHSO_4$ and $Cs_2S_2O_7$ caused by a partial thermal decomposition that includes the break-up of hydrogen bonds and the formation of H_2O molecules.

1. Introduction

Caesium hydrogen sulfate, $CsHSO_4$ (CHS), is considered to be the prototype salt of the $MeXAO_4$ (Me = Cs, Rb; X = H, D; A = S, Se) family, reportedly having a superprotonic-conducting phase at high temperatures [1]. In 1982, Baranov *et al* [1] found that, upon heating this salt through 141 °C, bulk conductivity increases drastically by several orders of magnitude to 10^{-2} S cm^{-1}. However, on the cooling run to room temperature, the conductivity of the low-temperature phase did not return to the values obtained when the crystal was first heated; instead, they were nearly half an order of magnitude higher than before (see figure 1 of [1]).

CHS exhibits three solid phases above room temperature. Herein, we have adopted the terminology used by Baranov *et al* [2] by which the low-, intermediate-, and high-temperature phases are denoted III, II, and I, respectively. At room temperature, phase III has a monoclinic symmetry with space group $P2_1/c$ [3]. This structure consists of zigzag chains of hydrogen bonds along the *b* axis of the crystal linking the SO_4 tetrahedral [4], resembling the CsH_2PO_4 (CDP) structure in the para-electric phase, except for the extra hydrogen in CDP [5]. At a given temperature between 57 and 97 °C, phase III transforms to phase II [6]. Recently, using

x-ray diffraction measurements, it has been observed that phase III still persists upon heating the sample up to 100 °C and from 90 °C gradually transforms to phase II [7]. The precise transformation temperature depends on details such as humidity, heating rate, and sample surface conditions [8]. Phase II has the same monoclinic symmetry and space group as that of phase III, but the unit-cell parameters change—leading to a smaller unit-cell volume [9, 4]. According to Belushkin *et al* [4], the zigzag chains of hydrogen bonds are present again in phase II but now along the *c* axis. In contrast with this conjecture, the III → II first-order transition has been interpreted on the basis of vibrational analysis [10–12], in terms of a conversion of infinite $(HSO_4^-)_n$ chains into cyclic $(HSO_4^-)_2$ dimers. Based on conductivity measurements, Badot and Colomban [13] found a clear decrease in conductivity at the III → II transition temperature and this behaviour was related to the formation of the cyclic dimers rather than infinite HSO_4 chains. Moreover, the reverse II → III transition does not take place when a sample is cooled [14]. But, this transformation occurs easily at room temperature, if the sample is kept in water vapour pressure above some threshold value (6.3 Torr at 20 °C) [14, 15]. The interpretation given for this observation [14] was that the absorption of water affects the orientation of the hydrogen bonds in a very thin layer at sample surface. At first, this change has little influence on the bulk, but when a certain fraction of the hydrogen bonds in this layer changes its orientation (along the *b* axis) it triggers an avalanche of reorientations that spread into the bulk. According to these authors, the reverse II → III transition could also be induced at room temperature by grinding the preheated CHS in a mortar [15]. In a polarized light study of CHS crystals, Kirpichnikova *et al* [16] reported a substantial decrease of crystal quality, and partial decomposition of the substance accompanied the III → II transition at 100 °C. The surface of the sample was covered with dark spots of a segregated substance. A subsequent measurement performed on the same specimen kept for two days at room temperature revealed that the temperature of the III → II transition decreased to 57 °C.

After further heating through 141 °C, CHS transforms into a superprotonic-conducting phase I [1, 2] which has a tetragonal symmetry with space group $I4_1/amd$ [4, 9, 17]. For the deuterated sample, $CsDSO_4$ (CDS), the transition temperature is 139 °C [2]. Therefore, the isotopic effect on the temperature phase transition is practically nil. In contrast to the lower-temperature phases (III and II), in phase I each SO_4 tetrahedron can adopt instead of one, four crystallographic-equivalent orientations [4]. Hence, the number of possible proton positions per unit cell becomes larger than the number of protons. Thus, the first-order phase transition to the superprotonic-conducting phase is triggered by an orientational disorder of the SO_4 tetrahedral, resulting in a rearrangement of the hydrogen bond network given the appearance of unfilled proton sites, allowing protons to move through the lattice by jumping to unfilled positions [4]. In others words, the principal mechanism for proton conduction is of Grotthuss-type, which takes into account tetrahedral reorientation and proton transfer [10]. Based on a molecular dynamic simulation [18], tetrahedral reorientation and proton transfer rates of the order of 10^{11} and 10^9 s^{-1}, respectively, were calculated. The anisotropic effect on the transition temperature has been explained because the transition is primarily driven by the disordering of the SO_4 tetrahedral, and proton disordering is a secondary effect [4]. Conversely, Jirak *et al* [19], Merinov *et al* [20], and Crisholm [21] assume only two crystallographic-equivalent orientations of the SO_4 tetrahedral. On the other hand, regarding the nature of proton transport in the low-conductivity phases (III and II), opposing points of view are reported by Hainovsky *et al* [22] and Norby *et al* [23]. Hainovsky *et al* [22] claim quantum tunnelling mechanisms for protons crossing the hydrogen bond barrier, while Norby *et al* [23] report that no anomalous isotope effects were observed, thus they found no support for proton tunnelling.

When the appearance of the CHS superprotonic plastic phase I is monitored by a polarization microscope, colour patterns unusual for monocrystals are observed [24].

Moreover, Kirpichnikova *et al* [16] also observed this phenomenon in the superprotonic-conducting phase of $CsDSO_4$ (CDS) crystals, but, upon cooling below 141 °C, a wedge-shaped ferroelastic domain structure was observed to grow through the motion of a phase front, the wedge-shaped structure became smaller, and the bright colour of the sample vanished [16]. Additionally, these authors observed that the II → I transition of CHS was also accompanied by a surface partial decomposition [16].

Furthermore, it has been reported [24] that the surface layer of CHS crystals undergoes a phase transition, accompanied by an appreciable increase in surface conductivity. This transition at 122 °C precedes the transition to the superprotonic-conducting phase at 141 °C. Baranov *et al* [24] suggest that the transition may be of the melting-solidification type of the surface layer with no more than a few unit cells of thickness. It is also indicated [24] that, when a CDS sample is held in moist air, a considerably higher surface conductivity is shown compared to that of a sample held in dry conditions. If the moistened sample is heated, conductivity values decrease to those of the dried sample.

It was also found that, above 203 °C, CHS decomposes according to the reaction [10, 25, 26]

$$2CsHSO_4 \rightarrow Cs_2S_2O_7 + H_2O \tag{1}$$

(displaying a broad differential scanning calorimetry peak between this temperature and 227 °C [10]) and, conversely, $Cs_2S_2O_7$ is hydrolyzed with water into $CsHSO_4$. Below this decomposition, some weight loss in the range from 0.02 to 0.15% was observed at 62, 107, 140, and 150 °C [11]. Colomban *et al* [11] concluded that weight modifications are connected to bulk defect formations, such as:

$$CsHSO_4 \leftrightarrow Cs(HSO_4)_{1-x}(S_2O_7)_{x/2} + \tfrac{1}{2}xH_2O, \tag{2}$$

$$CsHSO_4 \leftrightarrow \tfrac{1}{2}Cs_2SO_4 + \tfrac{1}{2}H_2SO_4, \tag{3}$$

$$CsHSO_4 + xH_2O \leftrightarrow CsHSO_4{\cdot}xH_2O \tag{4}$$

and that the easy formation of type (2) defects ($S_2O_7^{2-}$) and the sensitivity to water partial pressure at the II–I phase transition can strongly influence conductivity.

A 'proof-of-principle' demonstration of CHS as a proton exchange separator in fuel cells has been reported by Haile *et al* [27, 7]. Using Neumann and Kopp's law to calculate the formation energy of the condensed phases and the entropy changes of CHS at the III → II and II → I phase transitions, Uda *et al* [7] concluded that the electrolyte is thermodynamically stable up to 170 °C in a humidified oxygen atmosphere (0.03 atm H_2O) and that the mobile species are protons. On the other hand, from the electromotive force measurements generated across a sample of CHS placed in an oxygen concentration cell at 145 °C, a long time was required for the voltage to equilibrate (about 5 h), and at 129 °C the measurement voltage dropped to approximately −20 mV—significantly smaller than the theoretical value of −39.9 mV [7].

Finally, it is important to point out that the previously proposed phase transition to the superprotonic-conducting phase of CsH_2PO_4 (CDP) at 230 °C [28] has been claimed as not being of such a nature [29–32]. Instead, it has been assumed that the thermal anomaly, as well as the increase in conductivity observed round 230 °C, is a consequence of a chemical decomposition on the sample surface. Therefore, we decided to study the high-temperature phase behaviour of CHS by means of thermal analysis, impedance spectroscopy, and x-ray diffraction.

2. Experimental details

CHS dry, single crystals were grown by slow evaporation from an aqueous solution, prepared by mixing stoichiometric amounts of caesium carbonate, Cs_2CO_3, and sulfuric acid, H_2SO_4 [11]. The crystals were stored in a disector with silica gel.

Thermal gravi-metric analysis and differential scanning calorimetry (and modulated differential scanning calorimetry (MDSC)) measurements were performed by using TA-Instruments 2920 and TA-Instruments 2050 analysers, respectively. MS measurements were conducted by using a Balzers model Thermostar mass spectrometer. The heating rate used for these experiments was fixed to 2 °C min^{-1}, except for the MDSC experiment, where the average heating rate used was chosen to be 0.2 °C min^{-1}, and for the high-heating rate DSC experiment it was chosen to be 50 °C min^{-1}. 50 ml min^{-1} of dry nitrogen gas (with water content of about 5 ppm) was used as a purge gas for all these measurements, except for the differential scanning calorimetry (DSC) measurement, in which a 50 ml min^{-1} humidified nitrogen flux was used. The ac calorimetric technique [33] was used to measure the heat capacity of a single crystal in the form of a thin 0.1 mm-thick plate with an area of 2.5 mm^2.

The complex impedance was determined by means of a Hewlett Packard 4274A multi-frequency LCR meter. High-temperature x-ray powder diffraction patterns at different isotherms, from 25 to 175 °C, were taken using a Bruker-AXS D8 Advance x-ray diffractometer equipped with an Anton Paar HTK-1200 high-temperature furnace. These data were obtained using Kα radiation ($\lambda = 1.5406$ Å) with a 2θ scan step of 0.02° every 5 s. CHS crystals were gently crushed and ground into a powder using a mortar. The powder was used for both x-ray diffraction and impedance measurements. The powder for impedance measurements was pressed into pellets by using a steel die with a 10 mm diameter and uni-axial pressure of 6000 kg for 5 min. The electrodes of the 0.8 mm thick pellet were prepared with conducting silver paint. Conductivity was calculated from the frequency dependence of the real and imaginary parts of the impedance plots in the complex plane.

3. Results and discussion

The temperature dependence of the weight loss and the corresponding TG derivative curve for a dry CHS crystal are plotted in figure 1(a). The DSC curve for a dry CHS crystal and the conductivity data for a dry CHS pellet are plotted in figure 1(b). Since temperature scales for these data plots are the same, it is clear that all the DSC endothermic peaks at 61.5, 122.1, 141.5, and 200.3 °C fit well with the temperature derivative of the thermogravimetric curve (DTG) peaks, meaning that all the DSC endothermic peaks are associated with weight-loss steps. These steps are around 0.02, 0.03, 0.11, and 0.60%, respectively.

Moreover, our MS measurements on a dry CHS crystal (see figure 2) confirm the liberation of water molecules at 60, 122, 141, and 199 °C, indicating that dehydration reactions, such as those proposed previously [10, 11, 25, 26] (reactions (1) and (2)), could be taking place at these temperatures. Figure 3 reveals very similar experiments to those presented in figure 1. However, figure 3 shows the TGA and DSC data for dry samples constituted from a set of small crystals, including the ac calorimetric data for a thin, flat CHS crystal. The results presented in figure 3 show very clear weight-loss steps associated with the respective endothermic anomalies at 61.8, 121.0, and 141.6 °C. The weight-loss steps are around 0.08, 0.04, and 0.15%, respectively.

These values are higher than those of the single-crystal sample, indicating that the reaction takes place on the surface of the sample instead of through defect generation in the bulk (reaction (2)). Furthermore, this hypothesis is also supported by the observation that, at

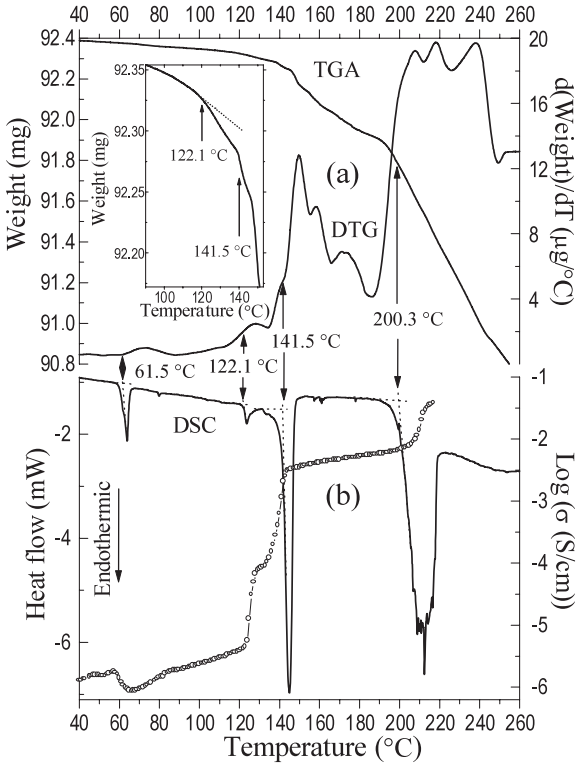

Figure 1. TGA, DSC and conductivity curves for dry CHS samp1es in the 40–260 °C temperature range. (a) TGA and its respective derivative curve, DTG, for a mono-crystalline sample. The inset amplifies the weight loss at the 90–153 °C temperature range. (b) DSC curve for a mono-crystalline sample and logarithmic conductivity curve for a pressed-pellet sample. Except for the inset, all plots have the same temperature scale. The heating rate for the TGA and DSC measurements was fixed to 2 °C min^{-1}.

the reported III → II transition, the surface of the sample is covered with dark spots of a segregated substance [16] and that the II → I transition is accompanied by a surface partial decomposition [16]. The unusual colour patterns observed [24] at phase I could be explained by the refraction of the polarized light at the water near the sample surface. Thus, our results support, upon heating CHS, a sequence of partial thermal decompositions according to reaction (1) takes place over the surface of the sample at around 60, 122, 141, and 200 °C, respectively.

Lee [29] has proposed, for the potassium dihydrogen phosphate family compounds, that partial thermal decomposition sets in round a characteristic temperature, T_p. By using these ideas, we believe that, in CHS, the kinetic course of the proposed solid-state decomposition is dominated by the initiation of localized reactions at particular localities and the subsequent advancement of a reactive interface into the non-decomposed reactant. This initiation occurs in the early stages of decomposition at, or very near, the crystal external surface at sites where crystallographic disorder exists. The crystal quality of the surface could be different, depending on its defect species, density, and distribution of the nucleation sites. The DSC anomaly at the relatively low temperature of 61.8 °C for a sample composed of several small crystallites (see figure 3(b)) compared to that of a single crystal (figure 1(b)) indicates that the temperature at which reaction (1) starts to take place at or very near the crystal surface of the sample depends on its particular quality in each specific crystallite. Therefore, this phenomenon could explain

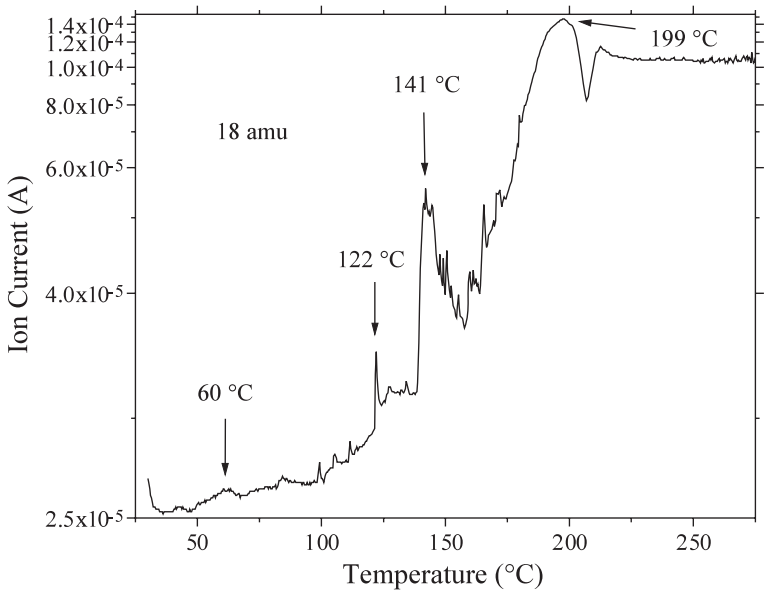

Figure 2. Temperature dependence of molecular water vapour concentration (ion current), measured by MS as evolved gas from a dry CHS crystalline sample heated at 2 °C min^{-1} in a coupled TGA apparatus.

why the reported III → II transition temperature is so widespread in the literature, as revised above for the various techniques used [6, 7, 9, 15, 16].

Concerning conductivity measurements at around 60 °C, some discrepancies are reported in the literature. While Baranov *et al* [1] reported that, upon heating a CHS crystal through this temperature, conductivity increased after an unusual peak, Badot and Colomban [13], who observed a reduction in conductivity, indicated that the conductivity increase observed by Baranov *et al* [1] is a consequence of the fixed-frequency method used by them. Our conductivity data for a CHS pellet show, upon increasing temperature, a small peak and then a decrease around 60 °C (see figure 1(b)). We believe that the unusual peak and the changes in conductivity, as well as the endothermic DSC peak, are consequences of the decomposition process at the surface of the samples, according to the reaction (1). Taking into account the previous observation that surface conductivity increases considerably when a dry deuterated CDS sample is placed in moist air [24] then heating a dry CHS sample through 60 °C, as a consequence of reaction (1), water is also present on the surface of the sample and the effect would be the same as when the sample is placed in a moist environment. In other words, the initially observed sharp increase in the CHS conductivity [1] is due to the presence of water at the surface of the salt, formed according to the reaction (1) and the dissolved part of it. However, almost immediately after the reaction (1) that takes place, initially at the most external surface layer, a thin solid crust of $Cs_2S_2O_7$ covers the surface (the same segregated substance observed by Kirpichnikova *et al* [16] at the III → II phase transition) and the resulting water may be partially evaporated. Therefore, electrical conductivity decreases and its final value depends on the amount or water released. This could explain both the unusual peak reported by Baranov *et al* [1] and the different changes observed in conductivity. If now the sample was cooled down, the reverse reaction

$$Cs_2S_2O_7 + H_2O \rightarrow 2CsHSO_4 \tag{5}$$

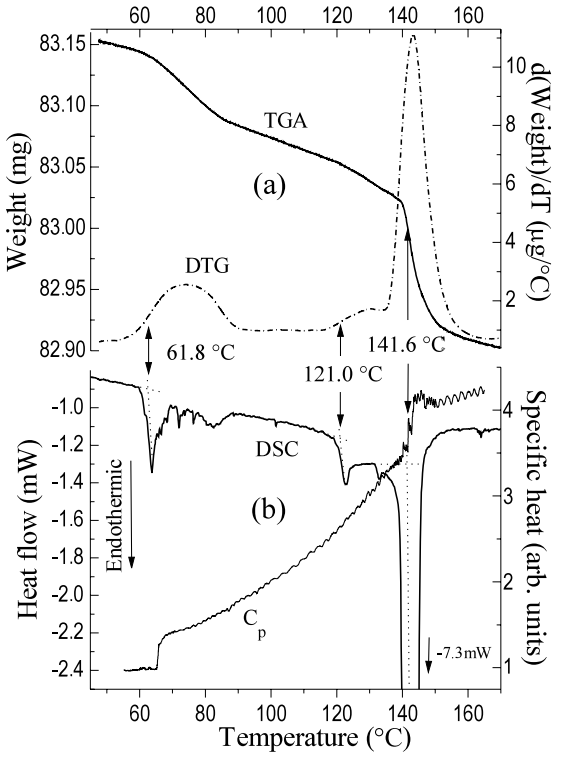

Figure 3. TGA, DSC and specific heat curves for dry CHS samples in the 45–170 °C temperature range. (a) TGA and its respective derivative curve, DTG, for a sample composed of a set of small crystals as they were grown, close to 0.5 mm^3 in volume. (b) DSC curve for a sample prepared as in (a), and specific heat curve for a small, thin, flat mono-crystalline sample. All plots have the same temperature scale. The heating rate for the TGA and DSC measurements was fixed at 2 °C min^{-1}.

would not take place, since the reverse DSC peak is not shown, probably because water is not sufficiently available either at the surface or in the surrounding atmosphere. In fact, only when the sample that was previously heated above 60 °C is exposed to a moist atmosphere at room temperature is the DSC peak at 60 °C shown again on the subsequent heating run [14, 15]. Similarly, this peak is also shown with the same intensity when the sample is heated from room temperature after removing the solid crust of $Cs_2S_2O_7$ formed on the surface of the sample by grinding it in a mortar [15].

We must point out that the conductivity data for the CHS pellet included in figure 1(b) is just for general discussion, because the TGA and DSC data correspond to crystalline samples. By heating the CHS pellet through 122 °C, its conductivity increases by about one and a half orders of magnitude and, upon further heating, a second jump on the conductivity starts to appear near 132 °C, finishing at 144 °C with conductivity values of about 4×10^{-3} S cm^{-1}. On further heating, the conductivity displays a final jump, starting at 200 °C and finishing at 217 °C, reaching values of about 4×10^{-2} S cm^{-1} (see figure 1(b)). Now, it has been reported that, above 203 °C, CHS decomposes according to reaction (1) [25, 26], revealing a broad DSC peak between this temperature and 227 °C [10]. This result agrees well with our DSC and TGA measurements, because the onset of the weight loss and the DSC peak at 200 °C correlate well with each other; see figure 1. On the other hand, it has also been reported recently that the

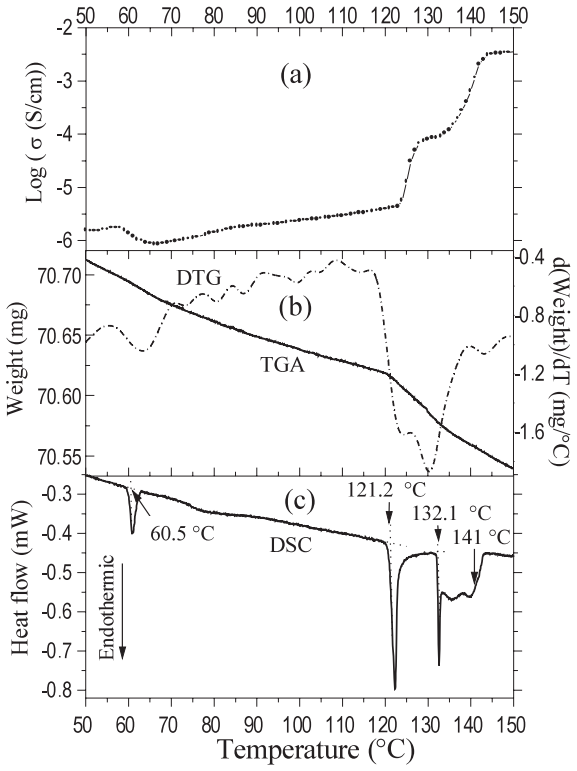

Figure 4. (a) Log σ curve for a dry pressed-pellet sample and (b) TGA and (c) DSC curves for two small CHS pellet piece samples in the 50–150 °C temperature range. The corresponding TGA derivative plot, DTG, is also plotted in (b). All plots have the same temperature scale. The heating rate for the TGA and DSC measurements was fixed at 2 °C min^{-1}.

melting point of CHS is at 218.5 °C [34]. Therefore, we believe that the conductivity jump, taking place between 200 and 217 °C, is perhaps a consequence of a strong decomposition process instead of the melting of the salt. This is supported not only by the strong weight loss that starts near 200 °C, but also by the very high liberation of water molecules above this temperature as measured by MS; see figure 2. Hence, we believe that quite a similar phenomenon is present for the lower decomposition stages at or very near the surface of the CHS crystals, reported here at 122 and 141 °C, respectively. Note, in figure 1, the coincidence of temperature values for all the onsets of weight-loss steps (TGA curves) with those of the corresponding DSC peak and step variations of the dc conductivity data.

The results presented in figure 4 correspond to dry CHS pellet samples. Conductivity data plotted in figure 4(a) correspond to that shown in figure 1(b), but in the 50–150 °C temperature range. The DTG curve, calculated from the derivative of the TGA curve, is also plotted in figure 4(b).

We note again that the weight-loss step and the conductivity changes observed near 60 °C correlate well with the DSC endothermic peak. The small weight loss observed for crystalline samples close to 122 °C is now more resolved. Moreover, the 122 °C TGA step is followed by additional weight loss around 132 °C, instead of that observed around 141 °C for the crystalline sample (see figures 1(a) and 3(b)), which is also shown by the DSC curve (figure 4(c)) and the dc conductivity data (figure 4(a)). Therefore, the transformation temperatures corresponding to

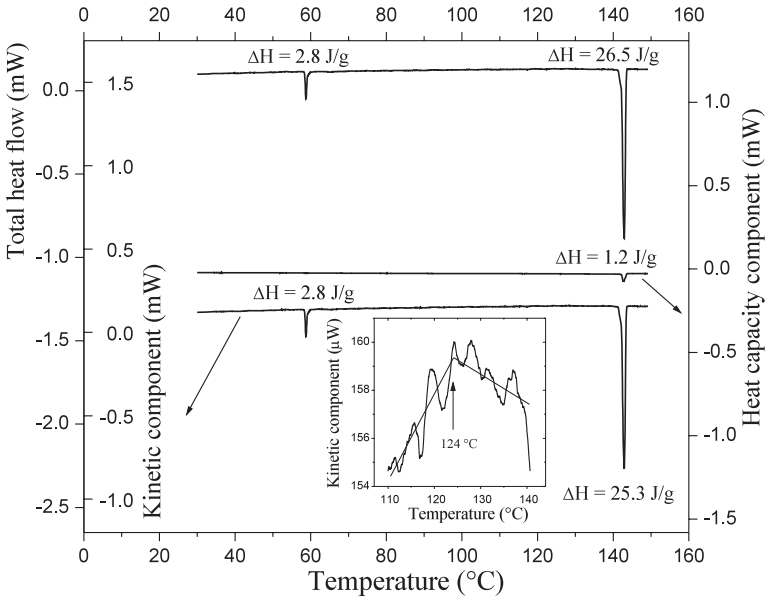

Figure 5. Total heat flow and its time-dependent (kinetic component) and time-independent (heat capacity component) components of a dry, small, thin, flat crystal with a mass of 10 mg, in the 30–150 °C temperature range. The heating rate was fixed at 0.2 °C min^{-1}. Except for the inset, all plots have the same temperature scale.

the DSC signals indicating all weight loss and conductivity variations are now better correlated when using samples with the same morphology.

The thermal results for a CHS single crystal in the 30–150 °C temperature range using the modulated DSC technique, which allows separation of the time-dependent (kinetic) component from the time-independent (heat capacity) component of the thermal response of the sample to a modulated heat flow [35], are shown in figure 5. Although the small DSC endothermic peak at 122 °C (see figure 1) is not well resolved in the MDSC curve, the inset shows—on an amplified scale of this region—a change in slope of the average base line of the kinetic component. MDSC results indicate that the enthalpy associated with the thermal events at around 60 and 141 °C, as measured from the kinetic component, correspond, respectively, to 100% (2.8 J g^{-1}) and 95.5% (25.3 J g^{-1}) of the total enthalpy values measured from the total heat flow signal.

Considering that decomposition reactions are time-dependent phenomena, the results suggest that 100% and 95.5% of the enthalpy anomalies at around 60 and 141 °C, respectively, are associated with these chemical processes. The remaining 4.5% of the total enthalpy measured for the heat capacity component (1.2 J g^{-1}) of the 141 °C MDSC peak could be associated with a physical transformation in the CHS crystals, similar to that claimed by Crisholm [21] for a superprotonic-conducting phase. However, the enthalpy associated with this transformation is much lower than the previously attributed value of 26.9 J g^{-1} [21]. As a matter of fact, when calculating the enthalpy change (from the configurational-entropy change) associated with the II → I phase transition due to reorientations of the SO_4 tetrahedral, Crisholm [21] concluded that only two instead of four orientations previously assumed [4] for the SO_4 are possible for the measured enthalpy. Consequently, from our MDSC measurements, the non-kinetic component of the enthalpy (1.2 J g^{-1}) cannot be related to a phase transition for a superprotonic-conducting phase of the CHS crystal at 141 °C.

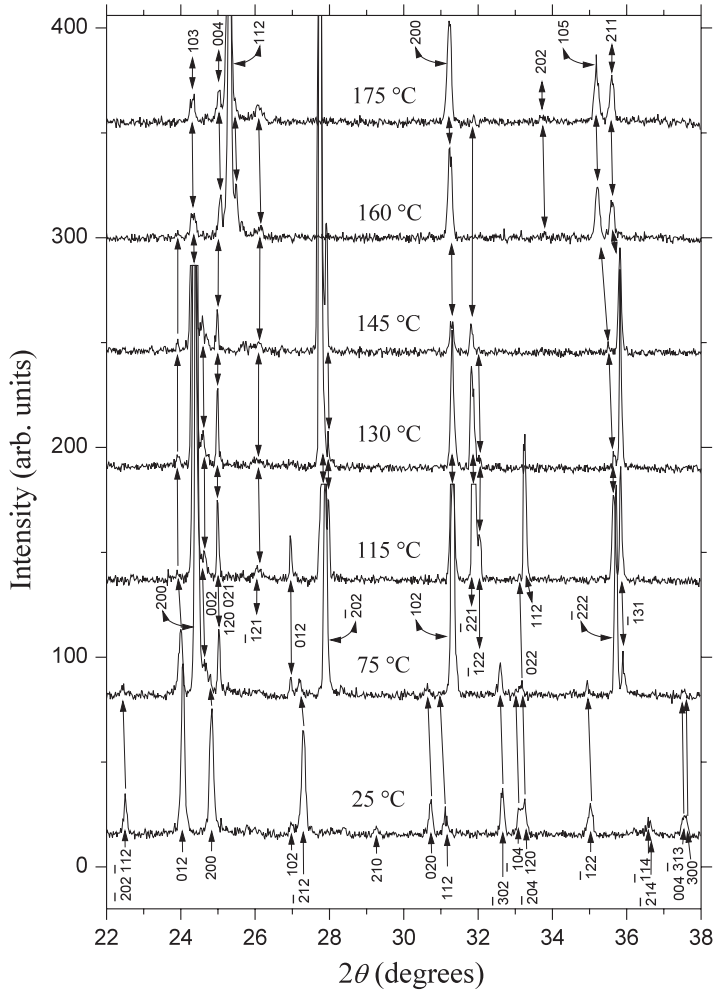

Figure 6. XRD patterns of CHS dry powder at 25, 75, 115, 130, 145, 160, and 175 °C, respectively. Miller indices assigned to the reflection peaks for the patterns obtained at 25, 75, and 175 °C are identical to those assigned to phases III, II, and I, respectively [3, 9]. The peaks for the 25 °C pattern that remain on subsequent high-temperature patterns and those new ones for the 75, 115, 160 and 175 °C patterns are marked with a single arrow and a double arrow, respectively.

As an additional test to support the chemical character of the reported III → II and II → I transitions of CHS, a high-heating-rate DSC measurement was also conducted on a dry, single crystal of CHS. While temperatures (enthalpies) for these thermal events were 58.8 °C (2.8 J g^{-1}) and 41.5 °C (26.5 J g^{-1}) at the low 0.2 °C min^{-1} heating rate, respectively, they were 81.8 °C (1.5 J g^{-1}) and 146.5 °C (18.8 J g^{-1}), respectively, at the high 50 °C min^{-1} heating rate.

Figure 6 shows high-temperature x-ray diffraction patterns of powdered CHS at several isotherms from 25 to 175 °C, under ambient air. The 25 °C diffraction pattern is identical to that reported by Itoh *et al* [3] for a monoclinic symmetry with space group $P2_1/c$ (phase III). Miller indices for the diffraction peaks were assigned according to reported data [3].

Comparing the 75 °C patterns to the 25 °C patterns, it is obvious that they are not identical to each other, but several peaks coincide with those reported by Nozik *et al* [9] at 57 °C (phase

II) and others with phase III. Thus, the 75 °C pattern shown in figures 6 may correspond to a two-phase coexistence (II + III) in which the new peaks have been indexed following the Nozik *et al* data [9] for phase II. However, the intensities of the $(\bar{1}21)$, $(\bar{1}22)$, $(\bar{2}21)$, and (112) diffraction peaks assigned to phase II only appear when the sample is heated up to 115 °C. The peaks of the 25 °C pattern that remain on subsequent high-temperature patterns and those new ones in the 75, 115, 160 and 175 °C patterns are marked with a single arrow and a double arrow, respectively. All the peaks from the 25 °C pattern are no longer present in the 130 °C pattern, except for the (012) peak that persist even in the 160 °C pattern. On the other hand, all the peaks assigned to phase II [9] (except for the (112)) also appear in diffractograms taken below (130 °C) and above (145 °C) the reported II → I phase transition temperature at 141 °C [1, 2]. Moreover, several peaks seemingly persist up to the 175 °C pattern where two new peaks appear around $2\theta = 25.32°$ and 33.71° in the 160 and 175 °C patterns. According to the x-ray data reported by Nozik *et al* [9], CHS at 157 °C has a tetragonal structure, phase I. Miller indices assigned to these peaks in the 175 or 160 °C patterns of figure 6 are those from [9] for phase I.

Since the III → II phase transition has been identified as a first-order phase transition [11], then the DSC results (see figures 1(b), 3(b), 4(c), and 5) would indicate that the coexistence of the III and II phases should only be possible at around 60 °C, contrary to the XRD results showing that peaks of phase III are also present in the 75, 115 and even 160 °C patterns. On the other hand, since the sample used in the TG measurement shown in figure 3 was formed from small crystallites, while that used in the XRD measurements was fine powder, the amount of $Cs_2S_2O_7$ formed at around 60, 121 and 141 °C was higher in the second experiment than in the first, given that the reaction (1) takes place at the surface of the crystals. Therefore, we believe that the 75 °C diffractogram corresponds to a sample with a two-phase composition: the CHS phase III and $Cs_2S_2O_7$, which appear as a segregated substance at the surface of the CHS powdered sample. Consequently, these results confirm that the III → II structural phase transition does not take place. On further heating of the sample, the remaining CHS (phase III) continues its decomposition to $Cs_2S_2O_7$. Comparing the 130 and the 145 °C diffractograms, except for the variation in the intensities of the peaks, it is clear that all the peaks (except the (012) of phase III) are present in both patterns and correspond to $Cs_2S_2O_7$. This assignment is reasonable because, around these temperatures, the amount of $Cs_2S_2O_7$ is much higher than 6% of the room temperature CHS sample and, since it is located over the surface of the crystallites, its absorption of the x-ray radiation is increased. Even at 160 and 170 °C, the sample may correspond to a phase mixture of CHS–$Cs_2S_2O_7$ and another phase yet to be identified. It is thus convincing that the x-ray patterns observed at 157 °C by Nozik *et al* [9] correspond to decomposition products of CHS but not to CHS. Therefore, we believe that the superprotonic-conducting tetragonal phase of CHS does not exist. However, if this interpretation were wrong, then, since the 130 and 145 °C patterns are essentially the same, it is reasonable to conclude that the II → I phase transition does not take place. Additionally, it is important to notice that the XRD patterns above 130 °C do show a shift of the $(\bar{2}22)$, and $(\bar{1}31)$ peaks to lower angles, which may be evidence of the plastic behaviour of the $Cs_2S_2O_7$–H_2O system.

Finally, in order to look at the effect of humidity upon the phase behaviour of CHS, DSC measurements were carried out on a crystalline sample under a humidified atmosphere created by using a 50 ml min^{-1} dry nitrogen flux mixed with a flux of 0.03 atm of water vapour. Results reveal an initial broad endodermic peak with an offset temperature at 42 °C followed by two endothermic peaks at 60.5 and 142.1 °C with enthalpy values of 2.6 and 24.6 J g^{-1}, respectively. The 42 °C offset peak corresponds to water released from the sample surface. The other two peaks are associated with the decomposition reaction (1). Therefore, it is concluded that the water vapour phase does not prevent decomposition. However, we have also observed that if a sample is arrested at any temperature between 60 and 141 °C and then cooled to

room temperature, then an exothermic effect appears, indicating that the water present in the environment reacts with the $Cs_2S_2O_7$ according to the reaction (5). It is also observed that when a CHS sample under a dry N_2 atmosphere is first heated from room temperature up to above 141 °C and then cooled to room temperature, an exothermic DSC peak occurs at around 136 °C, agreeing with the reported temperature value of the reverse I → II transition, obtained from conductivity measurements [1]. The DSC curve could be interpreted as follows: upon heating CHS through 60 °C, a thin solid crust of $Cs_2S_2O_7$ covers the surface, which hinders the progress of the reaction, but, upon subsequent heating through 141 °C, the reaction (1) continues its propagation inside the crystals (below the already formed crust of $Cs_2S_2O_7$) forming a liquid water phase. Recent results [34] of ^{133}Cs and ^{17}O nuclear magnetic resonance (NMR) and Raman spectra of the liquid $Cs_2S_2O_7$–$CsHSO_4$ system were interpreted by the presence of a temperature-sensitive equilibrium $2HSO_4^- \leftrightarrow S_2O_7^{2-} + H_2O$, where water molecules are strongly associated in the melting. Even though we have a solid $Cs_2S_2O_7$–$CsHSO_4$ system, it is probable that the water phase is strongly bound to $Cs_2S_2O_7$. So, although part of the water is released on heating the sample through 141 °C, as indicated by the TG measurements (see figures 1(a) and 3(a)), some other parts remain in the sample used for the hydrolysis, according to reaction (5) which occurs around 136 °C. The proposed scheme for the phase behaviour of CHS could also explain the observations reported in [7] (see above) when using it as an electrolyte separator for proton exchange at intermediate temperatures. The water in the cell dissolves part of the salt, providing protons to be conducted through the water embedded in the polymer (dimer) matrix.

In summary, our results support the concept that the CHS phase above 141 °C is not a superprotonic-conducting phase, but rather a mixture of $CsHSO_4$ and $Cs_2S_2O_7$ caused by partial thermal decomposition according to reaction (1). That is, the electrical conductivity mechanism above 141 °C for the CHS crystal includes the partial break-up of H-bonds and the formation of H_2O molecules at or near the surface of the crystal.

4. Conclusion

In summary, from the phase inter-relationships based on our TGA, MS, DSC, MDSC, ac calorimetric, x-ray diffraction, and impedance analyses, we propose that the high-temperature phenomena observed in CHS could be explained by a thermal-dehydration-like reaction (1) that takes place upon heating above room temperature. As a consequence, the endothermic effects and conductivity changes associated with the sequence of reported phase transitions in CHS—bulk phase transition III → II [1, 4, 7–9, 13, 15, 16], surface phase transition that leads to a high conductivity [24], and bulk phase transition to a superprotonic-conducting phase [1, 2, 4, 7, 9, 10, 16, 18–21, 24] close to 60, 122, and 141 °C, respectively—could be due to chemical decomposition processes at or very near the surface of the specimen.

Acknowledgments

This work was financed by the International Programme in the Physical Sciences, IPPS, of Uppsala University, Sweden, the Colombian Research Agency, COLCIENCIAS, and the Excellence Centre for Novel Materials, CENM.

References

[1] Baranov A I, Shuvalov L A and Shchagina N M 1982 *JETP Lett.* **36** 459–62
[2] Baranov A I, Shuvalov L A and Shchagina N M 1984 *Sov. Phys.—Crystallogr.* **29** 706

[3] Itoh K, Ukeda T, Ozaki T and Nakamura E 1990 *Acta Crystallogr.* C **46** 358–61
[4] Belushkin A V, Adams M A, Hull S and Shuvalov L A 1995 *Solid State Ion.* **77** 91–6
[5] Blinc R, Dolinsek J, Lahajnar G, Zupancic I, Shuvalov L A and Baranov A I 1984 *Phys. Status Solidi* b **123** K83–7
[6] Belushkin A V, Carlile C J and Shuvalov L A 1992 *J. Phys.: Condens. Matter* **4** 389–98
[7] Uda T, Boysen D A and Haile S M 2005 *Solid State Ion.* **176** 127–33
[8] Crisholm C R I and Haile S M 2000 *Mater. Res. Bull.* **35** 999–1005
[9] Nozik Yu Z, Lyakhovitskaya O I, Shchagina N M and Sarin V A 1990 *Kristallografiya* **35** 658–60
[10] Pham-Thi M, Colomban Ph, Novak A and Blinc R 1985 *Solid State Commun.* **55** 265–70
[11] Colomban Ph, Pham-Thi M and Novak A 1987 *Solid State Ion.* **24** 193–203
[12] Pham-Thi M, Colomban Ph, Novak A and Blinc R 1987 *J. Raman Spectrosc.* **18** 185
[13] Badot J C and Colomban Ph 1989 *Solid State Ion.* **35** 143–9
[14] Friesel M, Lundén A and Baranowski B 1989 *Solid State Ion.* **35** 91–8
[15] Lundén A, Baranowski B and Friesel M 1991 *Ferroelectrics* **124** 103–7
[16] Kirpichnikova L, Polomska M, Wolak J and Hilczer B 1997 *Solid State Ion.* **97** 135–7
[17] Belushkin A V, Carlile C J, David W I F, Ibberson R M and Suvalov L A 1991 *Physica* B **174** 268
[18] Münch W, Kreuer K D, Traub U and Maier J 1995 *Solid State Ion.* **77** 10–4
[19] Jirak Z, Dlouha M, Vratislav S, Balagurov A M, Beskrovnyi A I, Gordelii V I, Datt I D and Shuvalov L A 1987 *Phys. Status Solidi* a **100** K117
[20] Merinov B V, Baranov A I, Shuvalov L A and Maksimov B A 1987 *Kristallografiya* **32** 86
[21] Crisholm C R I 2003 *PhD Thesis* California Institute of Technology, Pasadena, CA, p 161
[22] Hainovsky N G, Pavlukhin Yu T and Hairetdinov E F 1986 *Solid State Ion.* **20** 249–53
[23] Norby T, Friesel M and Mellander B E 1995 *Solid State Ion.* **77** 105–10
[24] Baranov A I, Sinitsyn V V, Ponyatovskii E G and Shuvalov L A 1986 *JETP Lett.* **44** 237–40
[25] Simon A and Wagner H 1961 *Anorg. Allg. Chem.* **311** 103
[26] Walrafen G E, Irisii D E and Young T F 1962 *J. Chem. Phys.* **37** 662
[27] Haile S M, Boysen D A, Chisholm C R I and Merle R B 2000 *Nature* **410** 910–3
[28] Baranov A I, Khiznichenko V P and Shuvalov L A 1989 *Ferroelectrics* **100** 135
[29] Lee K S 1996 *J. Phys. Chem. Solids* **57** 333–42
[30] Ortiz E, Vargas R A and Mellander B E 1999 *J. Chem. Phys.* **110** 4847–53
[31] Ortiz E, Vargas R A and Mellander B E 1999 *Solid State Ion.* **125** 177–85
[32] Park J H 2004 *Phys. Rev.* B **69** 054104
[33] Jurado J F, Ortiz E and Vargas R A 1997 *Meas. Sci. Technol.* **8** 1151–5
[34] Rasmussen S B, Hamma H, Lapina O B, Khabibulin D F, Eriksen K M, Berg R W, Hatem G and Fehrmann R 2003 *J. Phys. Chem.* B **107** 13823–30
[35] Reading M, Elliott D and Hill V 1992 *Proc. 21st North American Thermal Analytical Society (Atlanta, GA)* pp 145–50